Chapter 28
On Elasto-Plastic Analysis of Thin Shells with Deformable Junctions

Jacek Chróścielewski, Violetta Konopińska and Wojciech Pietraszkiewicz

Abstract The non-linear equilibrium conditions for irregular thin shells are formulated from the appropriate form of the principle of virtual displacements. 2D constitutive relations of elasto-plastic behaviour of thin shells are established by dividing the shell into n layers and then integrating the corresponding 3D constitutive relations throughout all layers at each step of non-linear incremental solution by FEM. As example, deformation and stress states in the casing of pressure measuring devise are calculated taking into account deformability of the junctions.

Keywords Thin shell · Plasticity · Deformable junction · Finite element method · Casing

28.1 Introduction

In the recent paper by Chróścielewski et al. [1] we have proposed a methodology of the non-linear elasto-plastic analysis of thin shells with deformable junctions. The regular parts of the shell have been modelled by dividing the shell into n layers assumed to be in the plane stress state. The 3D incremental constitutive equations of each layer are described by the generalized elasto-plastic law of Prandtl-Reuss for small strains, with the associated flow rule and plasticity condition of Huber-Mises-Hencky with linear combination of isotropic and kinematic hardening.

J. Chróścielewski (✉) · V. Konopińska
Gdańsk University of Technology, Department of Structural Mechanics and Bridge Strctures, ul. G. Narutowicza 11/12, 80-952 Gdańsk, Poland
e-mail: jchrost@pg.gda.pl, violetta.konopinska@pg.gda.pl

W. Pietraszkiewicz
Institute of Fluid-Flow Machinery of the Polish Academy of Sciences, ul. Gen. J. Fiszera 14, 80-952 Gdańsk, Poland
e-mail: pietrasz@imp.gda.pl

H. Altenbach and V.A. Eremeyev (eds.), *Shell-like Structures*, Advanced Structured Materials 15, DOI: 10.1007/978-3-642-21855-2_28,

The 2D incremental constitutive equations for the shell stress resultants and stress couples are established by direct through-the-thickness integration throughout all layers of 3D relations mentioned above. The irregular shell with junctions are modelled according to Makowski et al. [2, 3] by a union of regular surface elements joined together along curvilinear surface edges, along which appropriate forms of 1D strain energy densities have been proposed. The methodology has been illustrated by numerical results of deformation and stress states in the casing of pressure measuring devise having two circular junctions between axisymmetric parts of different thickness. Only the limit cases of stiff and simply supported junctions have been analysed in [1].

In this report we first briefly remind basic non-linear relations of thin irregular shells with deformable junctions analysed within the elasto-plastic range of deformation. Then we present supplementary to [1] numerical results of deformation and stress states in the casing, where some intermediate cases of elastic junction behaviour defined by prescribed stiffness parameters are discussed.

28.2 Notation and Basic Relations

According to [2, 3], the consistent field equations and jump conditions of thin irregular shell structures can be derived using two postulates. In the kinematic one, the deformation of the irregular shell is assumed to be determined by stretching and bending of the irregular surface-like material continuum being a union of regular smooth surface elements $M^{(k)}$, $k = 1, 2, ..., K$, joined together along spatial curvilinear surface edges $\partial M^{(k)}$, which in the reference configuration are together denoted as M and Γ, respectively. Then the equilibrium conditions are required to be derivable from the principle of virtual displacements (PVD) involving only dynamic fields associated with the assumed kinematics of M. Such PVD is postulated in the form

$$G \equiv G_i - G_e - G_\Gamma = 0\,, \tag{28.1}$$

where G_i means the internal virtual work, G_e is the external virtual work, and G_Γ accounts for an additional virtual work of forces and couples acting only along all singular curves modelling the shell junctions.

Let $\mathbf{u}$ denote symbolically the translation field $\boldsymbol{u}$ inside all $M^{(k)} \in M$, the translation and rotation-like fields $(\boldsymbol{u}, \varphi)$ and $(\boldsymbol{u}_\Gamma, \varphi_\Gamma)$ along regular parts of $\partial M^{(k)}$ and Γ, respectively, the translation $\boldsymbol{u}_i$ at each corner $P_i \in \Gamma$, and the translation $\boldsymbol{u}_b$ at each corner $P_b \in \partial M$. Then after complex transformations given in detail in [3] we obtain

$$
\begin{aligned}
G(\mathbf{u};\delta\mathbf{u}) = &- \int\int_{M\setminus\Gamma} (\mathrm{Div}_s \boldsymbol{T} + \boldsymbol{l})\cdot\delta\boldsymbol{u}\, da \\
&+ \int_{\partial M_f} \{(\boldsymbol{p}_\nu - \boldsymbol{p}^* + \boldsymbol{k})\cdot\delta\boldsymbol{u} + (h-h^*)\delta\varphi\}\, ds \\
&+ \sum_{P_b\in\partial\bar{M}_f} \left\{[\boldsymbol{f}\cdot\delta\boldsymbol{u}]_b - \boldsymbol{f}_b^*\cdot\delta\boldsymbol{u}_b\right\} \\
&+ \int_{\partial M_d} \{(\boldsymbol{p}_\nu + \boldsymbol{k})\cdot\delta\boldsymbol{u} + h\,\delta\varphi\}\, ds + \sum_{P_b\in\partial\bar{M}_d} [\boldsymbol{f}\cdot\delta\boldsymbol{u}]_b \\
&+ \int_{\Gamma} \{([\boldsymbol{p}_\nu + \boldsymbol{k}] - \boldsymbol{f}_\Gamma)\cdot\delta\boldsymbol{u}_\Gamma + ([h] - h_\Gamma)\delta\varphi_\Gamma\}\, ds \\
&+ \sum_{P_i\in\bar{\Gamma}} \{[\boldsymbol{f}]_i - \boldsymbol{f}_i\}\cdot\delta\boldsymbol{u}_i = 0\,.
\end{aligned}
\tag{28.2}
$$

In (28.2), the compound tensor field $\boldsymbol{T}$ is defined in [3] through the surface symmetric stress resultant and stress couple tensors $\boldsymbol{N},\boldsymbol{M}$, the compound vector $\boldsymbol{l},\boldsymbol{p}_\nu,\boldsymbol{p}^*,\boldsymbol{k}$ and scalar h,h^* fields are defined in [3] through the external surface force $\boldsymbol{p}$ and moment $\boldsymbol{h}$ resultant vectors, acting on each deformed surface $\bar{M}^{(k)}$ but measured per unit area of $M^{(k)}$, as well as through the external boundary force $\boldsymbol{t}^*$ and moment resultant $\boldsymbol{h}^*$ vectors, prescribed along regular parts of the deformed boundary $\partial\bar{M}_f$ but measured per unit length of ∂M_f. Additionally, $\boldsymbol{f}_b^*$ are the external concentrated forces prescribed at each singular point $P_b\in\partial\bar{M}_f$, [...] means the jump of (...) along each regular part of Γ, $[...]_i$ is the jump of (...) at each singular point of Γ, $[...]_b$ means the jump of (...) at each singular point of ∂M, while δ is the symbol of variation and Div_s is the surface divergence operator.

For any kinematically admissible virtual displacement $\delta\mathbf{u}$ the fields $\delta\boldsymbol{u}$ and $\delta\varphi$ identically vanish along ∂M_d, so that the fourth row of (28.2) identically vanishes as well. Then the transformed PVD requires the equilibrium equations, the static boundary and corner conditions as well as the corresponding jump conditions along Γ to be satisfied. In such formulation the kinematic relations, the material and junction characterisation by the constitutive relations as well as the kinematic boundary conditions should additionally be specified.

The whole set of shell relations constitute the highly non-linear boundary value problem (BVP) in terms of translations and their surface gradients as the only independent field variables. This complex BVP can effectively be solved only by numerical methods applying some incremental-iterative solution procedure. The procedure is usually based on approximation of the non-linear BVP by series of linearised BVPs. For the Lagrangian non-linear theory of thin, regular elastic shells (without junctions) such solution procedure was worked out in [4], where the general structure of incremental shell equations and corresponding buckling shell equations were explicitly derived. However, in case of highly non-linear *irregular elasto-plastic* shell problems it is more efficient to apply the numerical incremental-iterative procedure directly to the incremental variational functional (28.2), not to the field equations following from it.

Let us briefly recall some statements of [4] and extend them to elasto-plastic shell problems with deformable junctions. Notice that components of the external loads in M, along ∂M_f and along Γ may be specified entirely independently, in general, by now 18 dimensionless parameters $\lambda_p \in \Lambda \subset \mathrm{R}^{18}$. Then the non-linear BVP for a thin irregular shell generated by (28.2) can be presented symbolically as $F(\mathbf{u}, \lambda_p) = 0$, where the non-linear continuously differentiable operator F is defined on the product space $C(M, E^3) \times \mathrm{R}^{18}$ with values in the Banach space, where $C(M, E^3)$ is a set of all components of $\mathbf{u}$ and its surface gradients up to the 4th order. In engineering applications all external loads are usually specified by a single common parameter $\lambda \in \Lambda \subset \mathrm{R}$. In this case the solution $\mathbf{u}(\lambda)$ of the BVP form a one-dimensional submanifold in $C(M, E^3)$ usually called the equilibrium path. $\mathbf{u}(\lambda)$ is called the weak solution if $G(\mathbf{u}(\lambda); \delta\mathbf{u}(\lambda)) = 0$ for all kinematically admissible $\delta\mathbf{u}(\lambda)$.

For finding the weak solution $\mathbf{u}(\lambda)$ one usually applies the Newton-Kantorovich method [5] based on successive approximations to the exact solution at some λ_{m+1} through solving a series of linearised BVPs following from linearisation of $G(\mathbf{u}(\lambda); \delta\mathbf{u}(\lambda)) = 0$ about a λ_m close to λ_{m+1},

$$G\left(\mathbf{u}_{m+1}^{(i)}; \delta\mathbf{u}\right) + \Delta G\left(\mathbf{u}_{m+1}^{(i)}; \Delta\mathbf{u}_{m+1}^{(i+1)}, \delta\mathbf{u}\right) = 0\,. \tag{28.3}$$

The first term in (28.3) represents the value of G at the approximation $\mathbf{u}_{m+1}^{(i)}$. Since this approximation may not belong to the equilibrium path, the first term in (28.3) does not vanish, in general, and allows one to calculate the unbalanced force vector at the configuration corresponding to $\mathbf{u}_{m+1}^{(i)}$. The second term in (28.3) linear with regard to $\Delta\mathbf{u}_{m+1}^{(i+1)}$ allows one to calculate the tangent stiffness matrix at $\mathbf{u}_{m+1}^{(i)}$ of the non-linear BVP. If $\mathbf{u}_{m+1}$ corresponds to the regular solution point then the successive approximations $\mathbf{u}_{m+1}^{(i+1)}$ established by this method converge to $\mathbf{u}_{m+1}$ with velocity of geometrical progression, provided that the initial approximation $\mathbf{u}_{m+1}^{(0)}$ is sufficiently close to $\mathbf{u}_{m+1}$.

The incremental shell relations following from (28.3) are valid for unrestricted translations, rotations, strains and/or bendings of the shell irregular base surface, arbitrary configuration-dependent external static loading, an arbitrary combination of work-conjugate boundary conditions, and arbitrary incremental constitutive relations of the shell and the junctions.

28.3 Constitutive Elasto-Plastic Modelling in Thin Shells

Analysis in the elasto-plastic range of deformation of thin irregular shells with deformable junctions can be performed by the finite element method with C^1 elements worked out by Nolte and Chroscielewski [6], which has been extended here to account deformability of the shell junctions. The shell is first divided into n layers and the plane stress state is assumed within each layer. The 3D incremental constitutive equations of each layer are described by the generalized elasto-plastic law of Prandtl-Reuss for small strains, with the associated flow rule and plasticity condition

of Huber-Mises-Hencky (HMH) with linear combination of isotropic and kinematic hardening.

In particular, in our constitutive shell model we apply the following relations:

1. Additive decomposition of differential increment of the Green strain tensor $\mathbf{e}$ into elastic and plastic parts,
$$d\mathbf{e} = d\mathbf{e}^E + d\mathbf{e}^P \,. \tag{28.4}$$
2. The overstress tensor,
$$\boldsymbol{\Sigma} = \mathbf{s} - \boldsymbol{\alpha} \,, \quad \boldsymbol{\Sigma}' = \mathbf{s}' - \boldsymbol{\alpha} \,, \quad \boldsymbol{\Sigma}' = \boldsymbol{\Sigma} - \tfrac{1}{3}\mathrm{tr}(\boldsymbol{\Sigma})\mathbf{I} \,, \tag{28.5}$$
where $\mathbf{s}$ is the 2^{nd} Piola-Kirchhoff stress tensor, $\mathbf{s}' = \mathbf{s} - \frac{1}{3}\mathrm{tr}\,(\mathbf{s})\,\mathbf{I}$ is its deviatoric part, $\boldsymbol{\alpha}$ is the corresponding back stress tensor, and $\mathbf{I}$ is the identity tensor of the 3D vector space.
3. The Huber-Mises-Hencky (HMH) yield condition,
$$f(\boldsymbol{\Sigma}, \bar{\varepsilon}^P) = \bar{\sigma} - \sigma_Y(\bar{\varepsilon}^P) = 0 \,, \quad \bar{\sigma} = \sqrt{\tfrac{3}{2}\boldsymbol{\Sigma}' : \boldsymbol{\Sigma}'} \,, \quad \frac{\partial f}{\partial \boldsymbol{\Sigma}} \equiv \mathbf{r} \,, \tag{28.6}$$
where $\bar{\sigma}$ is the HMH effective stress and σ_Y is the yield stress in uniaxial tension.
4. The associated plastic flow rule and evolution equation,
$$\begin{aligned} &d\mathbf{e}^P = (d\lambda)\,\mathbf{r} \,, \quad d\lambda = \frac{\mathbf{r} : \mathbf{C}^E : d\mathbf{e}}{H' + \mathbf{r} : \mathbf{C}^E : \mathbf{r}}, \quad d\bar{\varepsilon}^P = \sqrt{\tfrac{2}{3}\, d\mathbf{e}^P : d\mathbf{e}^P} \,, \\ &d\boldsymbol{\alpha} = (1-\beta)H' d\mathbf{e}^P, \quad d\sigma_Y = \beta H' d\bar{\varepsilon}^P \,, \end{aligned} \tag{28.7}$$
where $\mathbf{C}^E$ is the 4^{th}-order tensor of elastic moduli, $\bar{\varepsilon}^P$ is the accumulated effective plastic strain, H' is the strain hardening parameter, and $\beta \in [0, 1]$ is the material parameter determining proportion between isotropic and kinematic hardening.
5. The incremental constitutive relation of the elasto-plastic continuum,
$$d\mathbf{s} = \mathbf{C}^{EP} : d\mathbf{e} \,, \tag{28.8}$$
where $\mathbf{C}^{EP}$ is the instantaneous tangent 4^{th}-order tensor of the elasto-plastic material behaviour given by
$$\mathbf{C}^{EP} = \mathbf{C}^E - \frac{(\mathbf{C}^E : \mathbf{r}) \otimes (\mathbf{r} : \mathbf{C}^E)}{H' + \mathbf{r} : \mathbf{C}^E : \mathbf{r}} \,. \tag{28.9}$$

In this approach, as the hardening function we can also take the multi-segment approximation of experimental curves following from material tests in tension, if necessary. The stress increments corresponding to the strain increments are calculated from velocity relations using the Euler method of forward integration with correction following from the plasticity condition. Then the incremental constitutive equations for the shell stress resultants and stress couples are established by direct through-the-thickness integration throughout all layers of 3D relations mentioned above. All matrix relations for the finite element are calculated numerically

using 3-point Gauss integration within the element, and up to $n = 10$ integration points across the shell thickness are applied.

28.4 Deformation and Stress States in Axisymmetric Casing

The axisymmetric casing of measuring device being a part of a pressure installation consists of three regular thin shells of revolution: the circular cylindrical part of thickness h_c, length H and diameter D, and two toroidal parts of thickness h_s, inner boundary diameter d_z and radius r. These dimensions are related by $D = d_z + 2r$, see Fig. 28.1.

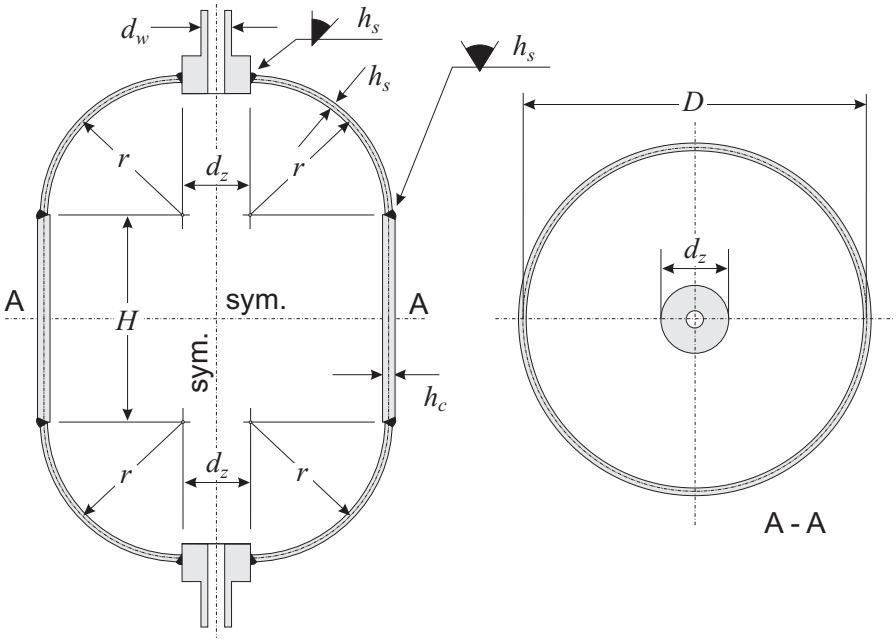

Fig. 28.1 The axisymmetric casing: geometry

The toroidal parts are connected with the cylindrical one by welding, while at the upper and lower ends the toroidal parts are connected with rigid parts by welding or screw joints. Thus, in this example we have different technological inaccuracies at the junctions associated with welding (or screw joints) and with change of thickness.

The force $P_{(a)}$ acting at the inner and lower toroidal boundaries, see Fig. 28.2, comes from pressure difference applied to rigid parts of the casing and is calculated according to

$$P_{(a)} = \frac{1}{4} q \pi \left(d_z^2 - d_w^2 \right). \tag{28.10}$$

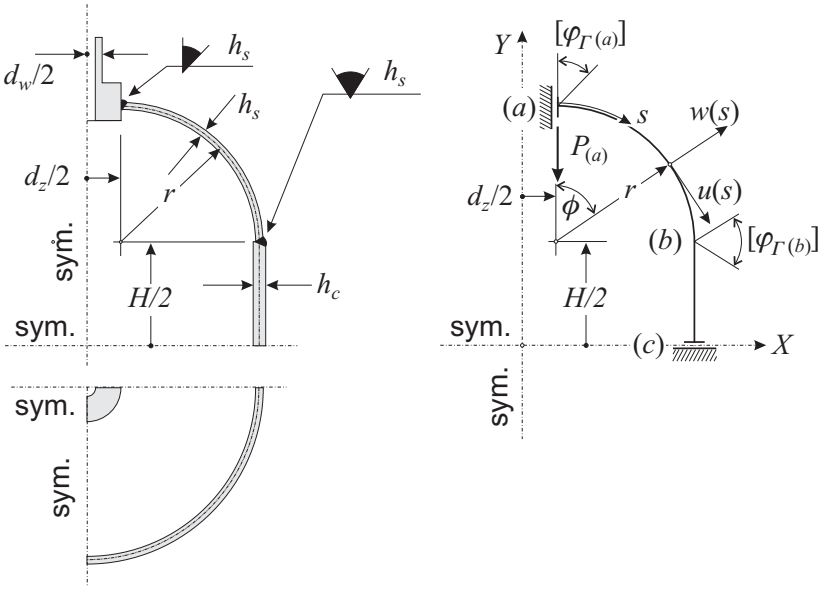

Fig. 28.2 The axisymmetric casing: scheme of analysis

In the numerical analysis of this example we use the program MINIMOD [6, 7] with the axisymmetric two-node RING element based on the theory of thin shells with finite rotations proposed in [8]. In this element two translation components u, w are approximated using the Hermite interpolation with C^1 interelement continuity of the form

$$\left\{\begin{matrix}\tilde{u}\\ \tilde{w}\end{matrix}\right\} = \sum_{k=1}^{2}\left(H_k^0 \left\{\begin{matrix}u_k\\ w_k\end{matrix}\right\} + H_{sk}^1 \left\{\begin{matrix}u,_{sk}\\ w,_{sk}\end{matrix}\right\}\right), \tag{28.11}$$

where H_k^0 and H_{sk}^1 are shape functions in the Hermite interpolation.

In the analysis the following numerical data have been used: $h_s = 1\,\text{mm}$, $H = 50\,\text{mm}$, $D = 100\,\text{mm}$, $d_z = 10\,\text{mm}$, $d_w = 5\,\text{mm}$, $r = 45\,\text{mm}$. Within the elastic range of deformation we take $E = 210\,\text{GPa}$ and $\nu = 0,3$. The plastic range of deformation is characterized by the initial plasticity limit $\sigma_0 = \sigma_Y(0) = 450\,\text{MPa}$, the mixed isotropic-kinematic hardening is described by the parameter $\beta = 1/2$ and the tangent modulus is taken as $E_T = 0,001 \times E$. The linear constitutive relation

$$\begin{aligned} &h_\Gamma = c\,[\varphi_\Gamma]\,, \quad c = c_{ref}\cdot\gamma\,, \quad c_{ref} = M_{0\Gamma}\cdot 2\pi r_\Gamma\,,\\ &M_{0\Gamma} = \frac{1}{4}\sigma_0 h_\Gamma\,, \quad \gamma \in [0,+\infty) \end{aligned} \tag{28.12}$$

governs deformability of the junctions.

Two values of the cylinder thickness h_c have been analysed with different values of the stiffness parameter c prescribed at the junctions.

1) $h_c = 2\,\text{mm}$

The numerical results for two extreme cases $c = 0$ and $c = \infty$ of the junctions (a) and (b) have been given in [1].

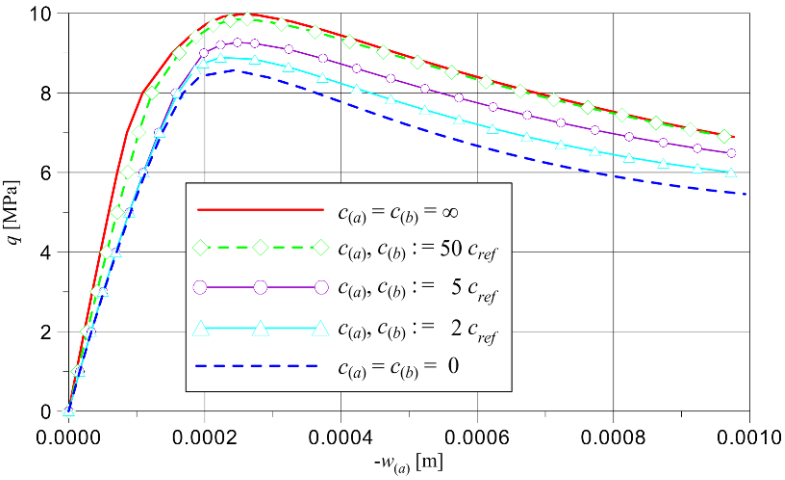

Fig. 28.3 Vertical translation of the point (a) as function of pressure and the junction stiffness

In Fig. 28.3 we present how the vertical translation $w_{(a)}$ depends on the external pressure q. With growing q the $w_{(a)}$ grows initially almost linearly up to about 6 MPa. Then for $q \in (6-8)\,\text{MPa}$ the plastic material behaviour makes the measurements of pressure less and less accurate. Above $q = 8\,\text{MPa}$ the graphs $w_{(a)} = f(q)$ become non-linear with clearly pronounced limit points for q above which the devise becomes damaged. The maximum value of the limit point corresponds to $c_{(a)} = \infty$, and its minimum value to $c_{(a)} = 0$. The values of $c_{(b)}$ have no noticeable influence on these results.

In Fig. 28.4 we show how the angle of rotation φ changes along $s/L \in [0, 1]$, $L = 1/4\,(H + \pi r)$. When both junctions at (a) and (b) are stiff, i.e. $c_{(a)} = c_{(b)} = \infty$, the relative rotation at these points becomes zero and the graph has no jumps, see [1]. For both simply supported junctions, i.e. $c_{(a)} = c_{(b)} = 0$, as well as for the finite stiffness of $c_{(a)}$ and $c_{(b)}$ there are two jumps of the graph at the junctions, but this effect is pronounced only locally.

In Fig. 28.5 it is shown how the bending couple M^1 along the casing meridian for $q = 8\,\text{MPa}$ is distributed. It is seen that for $c_{(a)} = c_{(b)} = 0$ there are zero values of the couple at both junctions. The stiffness parameters of either junction has only local effect, and for all non-zero stiffness values the couple between the toroidal and cylindrical parts of the casing is very mall.

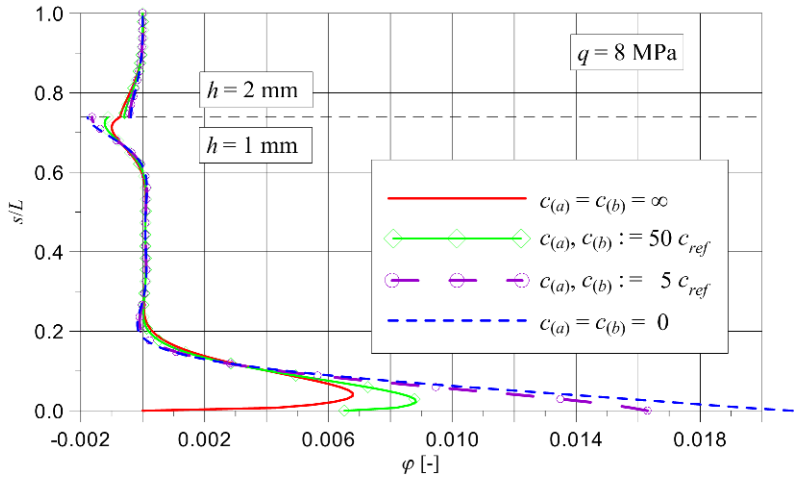

Fig. 28.4 Angle of rotation along the casing meridian for $q = 8\,\text{MPa}$

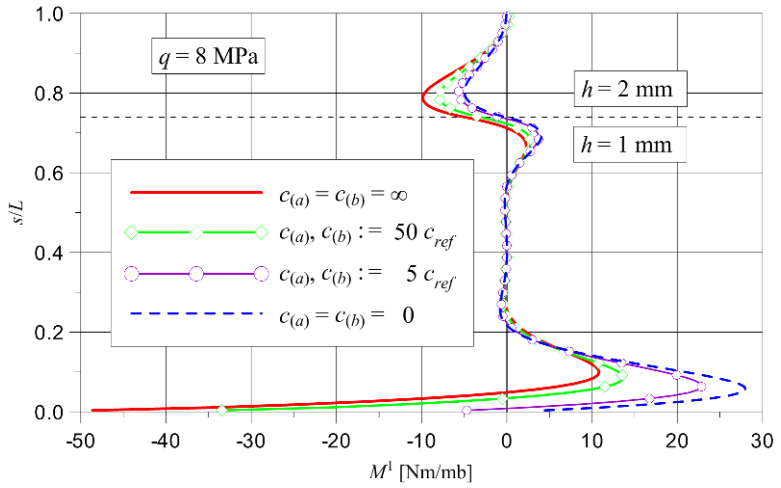

Fig. 28.5 Bending couple along the casing meridian for $q = 8\,\text{MPa}$

2) $h_c = 1\,\text{mm}$

Similar numerical simulations as above performed for the cylindrical thickness $h_c = 1\,\text{mm}$ are given in Figs 28.6–28.8. Although the cylinder thickness here is only half of that discussed in the case 1), the overall deformability of the casing is almost the same as above.

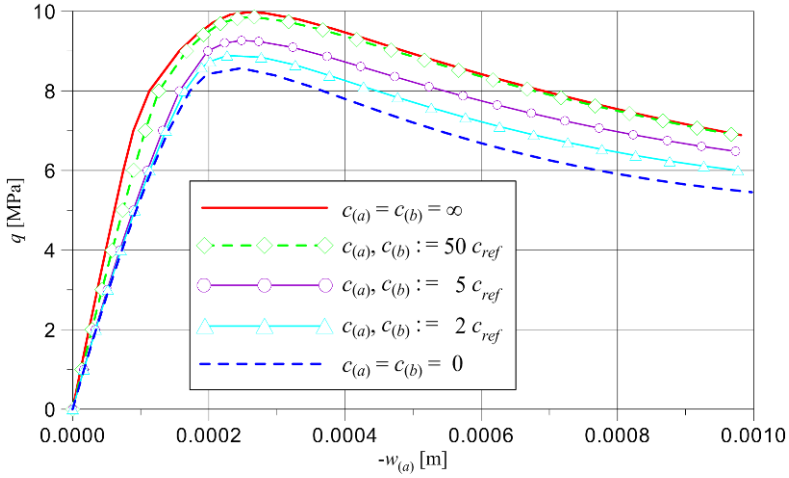

Fig. 28.6 Vertical translation of the point (a) as function of pressure and the junction stiffness

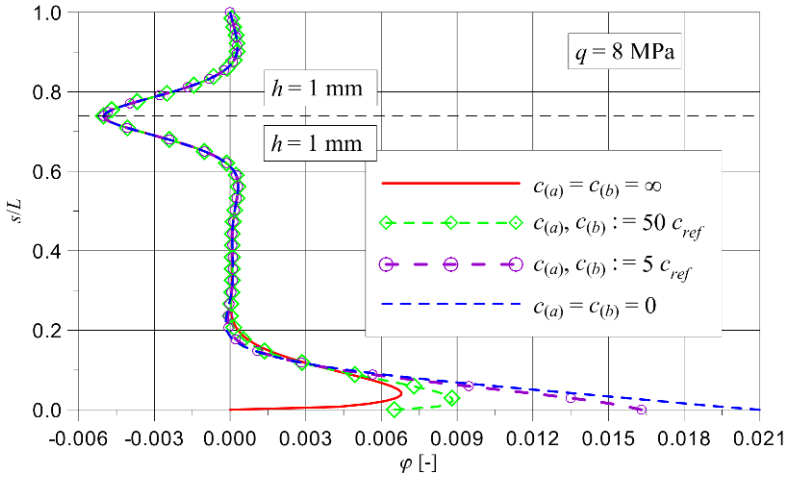

Fig. 28.7 Angle of rotation along the casing meridian for $q = 8$ MPa

From the results of 1) and 2) the following behaviour of the casing can be observed:

- The overall axisymmetric carrying capacity of the casing depends primarily on plastification of its toroidal part near the junction (a).
- Disturbances of deformation and stress states due to the junctions (a) and (b) are local without noticeable influence on each other.
- In case 2), the shell rotations on both sides of (b) are almost the same and practically independent on the junction stiffness. However, for different thicknesses discussed in case 1), these rotations become distinct and their difference depends on the junction stiffness.

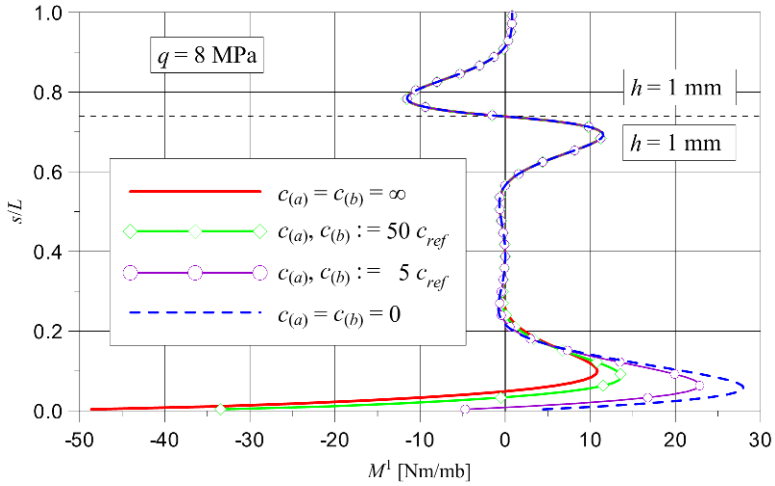

Fig. 28.8 Bending couple along the casing for $q = 8$ MPa

28.5 Conclusions

We have presented a refined formulation of the principle of virtual displacements for modelling of thin irregular elasto-plastic shells with elastic junctions. The 2D constitutive relation in the interior shell domain have been established by dividing the shell into n layers and then integrating the corresponding 3D constitutive relations throughout all layers at each step of non-linear incremental solution by the FEM. We have applied the C^1 axisymmetric finite element of [6] and calculated numerically the deformation and stress states in the casing of pressure measuring devise with two circular junctions. As compared with [1], several additional values of the junction stiffness and two values of thickness of the cylindrical part have been taken into account. The influence of junction stiffness on the results have been analysed.

Acknowledgements The research was supported by the Polish Ministry of Science and Education under grant No N 506 254237.

References

1. Chróścielewski, J., Konopińska, V., Pietraszkiewicz, W.: On modelling and non-linear elasto-plastic analysis of thin shells with deformable junctions. ZAMM **91**, 6, (2011) (in print)
2. Makowski, J., Pietraszkiewicz, W., Stumpf, H.: On the general form of jump conditions for thin irregular shells. Arch. Mech. **50**, 2, 483–495 (1998)
3. Makowski, J., Pietraszkiewicz, W., Stumpf, H.: Jump conditions in the non-linear theory of thin irregular shells. J. Elasticity **54**, 1, 1–26 (1999)
4. Pietraszkiewicz, W.: Explicit Lagrangian incremental and buckling equations for the non-linear theory of thin shells. Int. J. Non-Linear Mech. **28**, 2, 209–220 (1993)

5. Krasnosel'skii, M.A., Vainikko, G.M., Zabrejko, P.P., Rutitskii, Ya.B., Stetsenko, V.Ya.: Approximate Solutions of Operator Equations. Wolters-Nordhoff Publ., Groningen (1972)
6. Nolte, L.-P., Chroscielewski, J.: Large rotation elastic-plastic analysis of flexible shells. In: Taylor, C. et al. (eds.), Numerical Methods for Non-Linear Problems, Vol. **3**, pp. 391–404. Pineridge Press, Swansea (1986)
7. Chróścielewski, J., Branicki, Cz.: MINIMOD – Pakiet podprogramów wspomagający badanie zagadnień nieliniowych. W: Mater. IX Konf. „Metody Komputerowe w Mechanice", tom **1**, str. 131-138. Kraków-Rytro (1989)
8. Pietraszkiewicz, W., Szwabowicz, M.L.: Entirely Lagrangian nonlinear theory of thin shells. Arch. Mech. **33** , 273–288 (1981)